Available online at www.sciencedirect.com
ScienceDirect
Journal of Solid State Chemistry 180 (2007) 2189–2193
JOURNAL OF SOLID STATE CHEMISTRY
www.elsevier.com/locate/jssc

Ordered tetragonal spinel $LiMnNbO_4$ prepared in reducing atmosphere

I.L. Shukaev*, A.A. Pospelov, A.A. Gannochenko

Faculty of Chemistry, Southern Federal University, 7 ul. Zorge, Rostov-on-Don, 344090 Russian Federation

Received 13 February 2007; received in revised form 14 May 2007; accepted 22 May 2007
Available online 29 May 2007

Abstract

$LiMnNbO_4$, the first quaternary compound in Li–Mn–Nb–O system, has been prepared by solid-state reaction in hydrogen atmosphere at 1050 °C. According to the X-ray Rietveld refinement results ($R(F^2) = 0.0265$, $\chi^2 = 2.765$), it is isostructural with $LiZnNbO_4$: tetragonal, $P4_322$, $a = 6.1858(1)$, $c = 8.5312(1)$ Å, $Z = 4$, spinel-derived, with Li and Nb ordered on octahedral sites and with Mn in tetrahedral coordination.

Keywords: Ordered spinel; Lithium manganese(+2) niobate

1. Introduction

This paper reports the first investigation of Li_2O–MnO–Nb_2O_5 system. Previously, only one unsuccessful attempt to obtain $LiMnNbO_4$ in air was described [1]. But it is well known that complex oxides containing manganese (+2) may be readily prepared in reducing or inert atmosphere. Only $LiNbO_3$-based solid solutions $Li_{1-3y}Nb_{1-y}Mn_4^{+2}{}_yO_3$ were earlier described [2]. Phases like this, containing Li and a low-valence transition metal, may take part in solid state redox processes and, hence, be useful for electrochemical devices. In addition, any new compound may be of general interest, for example, aiming to detail the conditions of different structure types stability.

In the analogous Li_2O–ZnO–Nb_2O_5 system, the compound $LiZnNbO_4$ was first described by Blasse [1] and then the suggested structure was confirmed [3–5]. It is spinel-derived: Li and Nb are ordered on octahedral sites and Zn occupies tetrahedral sites. Two other ternary oxides and a wide range of cation-deficient solid solutions based on $LiZnNbO_4$ were found later [6]. The solid solution region extends towards the $Zn_3Nb_2O_8$ compound having a spinel-related structure (monoclinic superlattice with cation deficiency)—up to $y = 0.5$ in $Li_{1-y}Zn_{1+y/2}NbO_4$ formula. Electrical conductivities of these solid solutions and of pure $LiZnNbO_4$ are very low (no more than 5×10^{-5} S/m at 300 °C for ceramic samples) [6].

It is well known that Zn^{+2} and high-spin Mn^{+2} are very similar in their coordination preferences due to lack of crystal field effects and proximity of the ionic radii (0.74 and 0.80 Å, respectively, in tetrahedral surrounding [7]). Hence, an analogy between the two systems is expected, in particular, formation of $LiMnNbO_4$ compound.

2. Experimental

The starting substances were Mn_2O_3, Nb_2O_5 and Li_2CO_3, all of analytical grade. Manganese oxide was calcined in the Mn_2O_3 thermal stability range (700–750 °C) up to stable mass, niobium oxide was calcined at 900 °C and lithium carbonate was dried at 200 °C.

Solid state synthesis technique was used; reducing atmosphere (hydrogen) was chosen to stabilize Mn^{+2}.

Firstly, Li_3NbO_4 was synthesized in air. The lithium carbonate (with 2% excess, this correction takes into account the Li_2O volatility) and Nb_2O_5 were ground in agate mortar, pressed into 5–6 g pellets and calcined in air twice (at 700–800 and 900–950 °C, with intermediate regrinding). Using of presynthesized lithium niobate (instead of carbonate) strongly lowers the gas formation at the final synthesis stage and, thus, may help attaining equilibrium. The kinetics is better with starting Li_3NbO_4 than with more inert $LiNbO_3$.

*Corresponding author.
E-mail addresses: ishukaev@rsu.ru, ishukaev@mail.ru (I.L. Shukaev).

0022-4596/$ - see front matter © 2007 Elsevier Inc. All rights reserved.
doi:10.1016/j.jssc.2007.05.020

Thin powders of Mn_2O_3, Nb_2O_5 and Li_3NbO_4 were ground together in the desired ratio and pressed into pellets of 1.5–3 g of mass. The principal synthesis stage was performed in the tubular electrical furnace in hydrogen with flowing rate near 1 l/h. The hydrogen was passed over the copper granules heated up to 600 °C to eliminate the oxygen traces and then through the concentrated H_2SO_4 and KOH granules for drying. Pellets wrapped in nickel foil were heated up to 1020–1050 °C in one hour and then kept at this temperature for 5 h. Although hydrogen was dried prior use, small amounts of water vapour resulted from reduction of Mn_2O_3 and effectively suppressed reduction of Nb^{+5}, as evidenced by light coloration of the product. To prevent possible phase changes on cooling, the reaction tube was quenched in air off the furnace.

X-ray phase analysis at all stages was performed with a DRON-2.0 diffractometer using Ni-filtered CuKα-radiation. Single-phase pattern for structure analysis was measured utilizing a Geigerflex *D*/max-RC instrument equipped with a secondary-beam graphite monochromator. About 20 wt.% instant coffee powder was admixed to the sample to reduce grain orientation effect. For the Rietveld refinement, GSAS + EXPGUI suite [8,9] was used.

3. Results and discussion

3.1. Phase formation

The product after synthesis and grinding is a grayish-yellow powder slowly darkening in air without significant change of X-ray powder pattern. It is slightly hygroscopic and is stored in a dry hydrogen-filled desiccator. Darkening may correspond to the oxidative lithium deintercalation (with $Li_{1-x}Mn^{+2}_{1-x}Mn^{+3}_{x}NbO_4$ product). Possible hydrolysis probably corresponds to the lithium substitution (with $Li_{1-x}H_xMnNbO_4$ product).

The pattern of $LiMnNbO_4$ composition (Fig. 1) is very similar to that for previously described $LiZnNbO_4$ [10, card 00-023-1206] with a slight shift to lower angles, in agreement with greater ionic radius of Mn^{+2}.

Taking into account the analogy between these compounds and using the same technique as for pure $LiMnNbO_4$, the compositions of supposed $(Li_{1-y}Mn_{y/2})MnNbO_4$ solid solutions were prepared. But even at small y (near 0.02), X-ray patterns clearly show $Mn_4Nb_2O_9$-type phase [11] impurity, and with increasing y, $MnNb_2O_6$-type phase [12] also appears. Possibly, these are lithium-containing solid solutions rather than pure manganese (+2) niobates, but we did not check this opportunity.

3.2. Structure refinement

The increase in cell volume (Table 1) correlates with ionic radii difference for Zn^{+2} and Mn^{+2}. Both phases have spinel-like pseudo-cells, which are slightly flattened along the tetragonal axis ($c/a < \sqrt{2} = 1.414\ldots$).

As starting model we used the refined with internal standard (NIST SRM 676 corundum powder) tetragonal parameters of $LiMnNbO_4$ and atomic coordinates of $LiZnNbO_4$ from the most precious single crystal XRD and powder ND data [3,6]. We used the completely ordered model and Mn^{+2} instead Zn^{+2}. Initially, displacement parameters were isotropic and equal to 0.025. For new

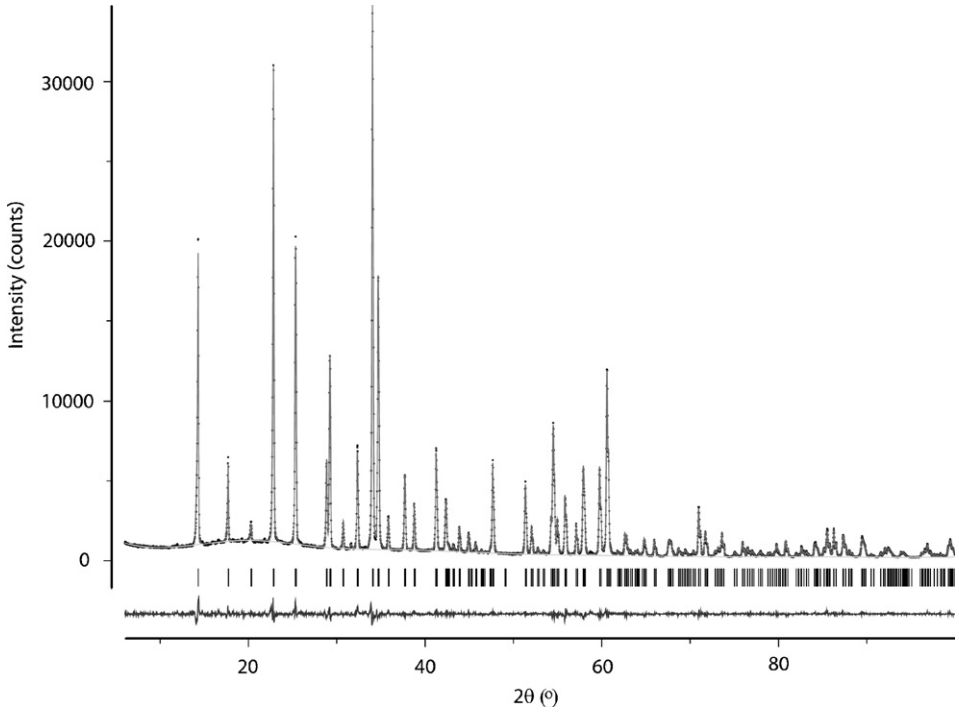

Fig. 1. Experimental (stars), calculated (line) and difference (bottom) X-ray powder diffraction profiles for $LiMnNbO_4$.

compound, the $P4_322$ space group was chosen between the two enantiomorphs of $LiZnNbO_4$, as in [3].

Using the GSAS package, the following variables were refined: two tetragonal lattice parameters, from two up to 20 background parameters, 11 parameters of peaks shape, nine independent atomic coordinates, four isotropic and four anisotropic displacement parameters, one or two occupation parameters (Li–Mn inversion), two angular shift parameters, one parameter of preferred orientation (texture).

After optimization of peak shape and background, cell parameters and shift data, two variable coordinates of Nb and Mn were refined. Then we operated with seven variable oxygen and lithium coordinates, interleaving cycles with profile parameters and heavy atoms coordinates. At the next stage displacement parameters were also refined. We also had taken into account a slight texturing of sample. For the preferred orientation correction the March–Dollase formulation [9] was used with [0 0 1] cylinder axis. The optimum found was $\chi^2 \sim 3$ and $R(F^2) \sim 0.029$.

Finally, the Li–Mn inversion in 4*c* ($Mn_{1-x}Li_x$) and 4*a* (Mn_yLi_{1-y}) was checked, as scattering factor of Mn is many times larger than that of Li. We checked both cases ($x = y$ and $x \neq y$). Li or Mn mixing with Nb was neglected. Both approaches give similar results, showing a small, if

Table 4
Selected interatomic distances (Å) in $LiMnNbO_4$

$Li_{0.981}Mn_{0.019}$–O	$Mn_{0.981}Li_{0.019}$–O	Nb–O
Average ionic radii sum [7]		
2.0370 × 2	2.0566 × 2	1.8364 × 2
2.2063 × 2	2.0629 × 2	1.9767 × 2
2.3234 × 2		2.1496 × 2
2.189	2.060	1.988
2.14	2.04	2.02

Table 1
Lithium-containing tetragonal spinel-derived niobates

Compound	S.G.	*a* (Å)	*c* (Å)	*c*/*a*	*V* (Å^3)	Technique	Refs.
$LiZnNbO_4$		6.085	8.400	1.381	311.0	XRD, powder	[6]
$Li_{1/2}Zn_{5/4}NbO_4$		6.116	8.380	1.370	313.5	XRD, powder	[6]
$LiZnNbO_4$	$P4_322$	6.0804	8.3988	1.3813	310.51	ND, powder	[3]
$LiZnNbO_4$	$P4_122$	6.082	8.403	1.382	310.8	XRD, powder	[4]
$LiZnNbO_4$	$P4_122$	6.082	8.382	1.378	310.1	XRD, single crystal	[5]
$LiMnNbO_4$	$P4_322$	6.1858	8.5312	1.3792	326.44	XRD, powder	This work

Table 2
Details of Rietveld refinement for $LiMnNbO_4$

Crystal system		Tetragonal	Density (calc.)		4.45
Space group		$P4_322$ (no. 95)			
Lattice constants (Å)	*A*	6.1858(1)	2Θ range (°)		6.00–99.98
	C	8.5312(1)	Step width (°)		0.02
Cell volume (Å^3)		326.44(1)	No. of data points		4700
Formula weight		218.78	No. of reflections		126
Z		4	No. of variables		62 (20—of structure)
Wavelengths (Å)	α_1	1.5406	Agreement factors	$R(F^2)$	0.0265
	α_2	1.5444		R_{wp}	0.0486
	Ratio	0.5		χ^2	2.765

Table 3
Atomic coordinates and displacement parameters for $LiMnNbO_4$

Atom	Site	Occ.	*x*	*y*	*z*	U_{iso}
Li_1	4*a*	0.981	0.221(1)	0	1/4	0.018(2)
Mn_1	4*c*	0.981	0.2555(1)	0.2555(1)	5/8	0.0122(2)
Nb_1	4*b*	1	1/2	0.22204(9)	0	
O_1	8*d*	1	0.2708(3)	0.0335(3)	0.9951(2)	0.0187(7)
O_2	8*d*	1	0.2697(3)	0.4806(3)	0.0213 (2)	0.0142(7)
Li_2	4*c*	0.019	0.2555(1)	0.2555(1)	5/8	0.0122(2)
Mn_2	4*a*	0.019	0.221(1)	0	1/4	0.018(2)
	U_{11}	U_{22}	U_{33}	U_{12}	U_{13}	U_{23}
Nb_1	0.0084(3)	0.0095(3)	0.0099(3)	0	0.0010(4)	0

Table 5
Bond valence sums in $LiMnNbO_4$

Position label	Wyckoff symbol	Occupations	Formal valence	BVS	Delta	%
Li_1	4*a*	Li^{+1}(0.981)	1.019	0.919	−0.100	9.8
Mn_2		Mn^{+2}(0.019)				
Mn_1	4*c*	Mn^{+2}(0.981)	1.981	1.908	−0.073	3.7
Li_2		Li^{+1}(0.019)				
Nb_1	4*b*	Nb^{+5}(1)	5.000	5.171	0.171	3.4
O_1	8*d*	O^{-2}(1)	2.000	2.054	0.054	2.7
O_2	8*d*	O^{-2}(1)	2.000	1.944	−0.056	2.8

For "mixed" positions 4*a* and 4*c* we took into account the occupations p_1 and p_2 of two kinds atoms: $v_{ij} = p_1 \exp((d_{ij}-L_1)/b)+p_2 \exp((d_{ij}-L_2)/b)$.

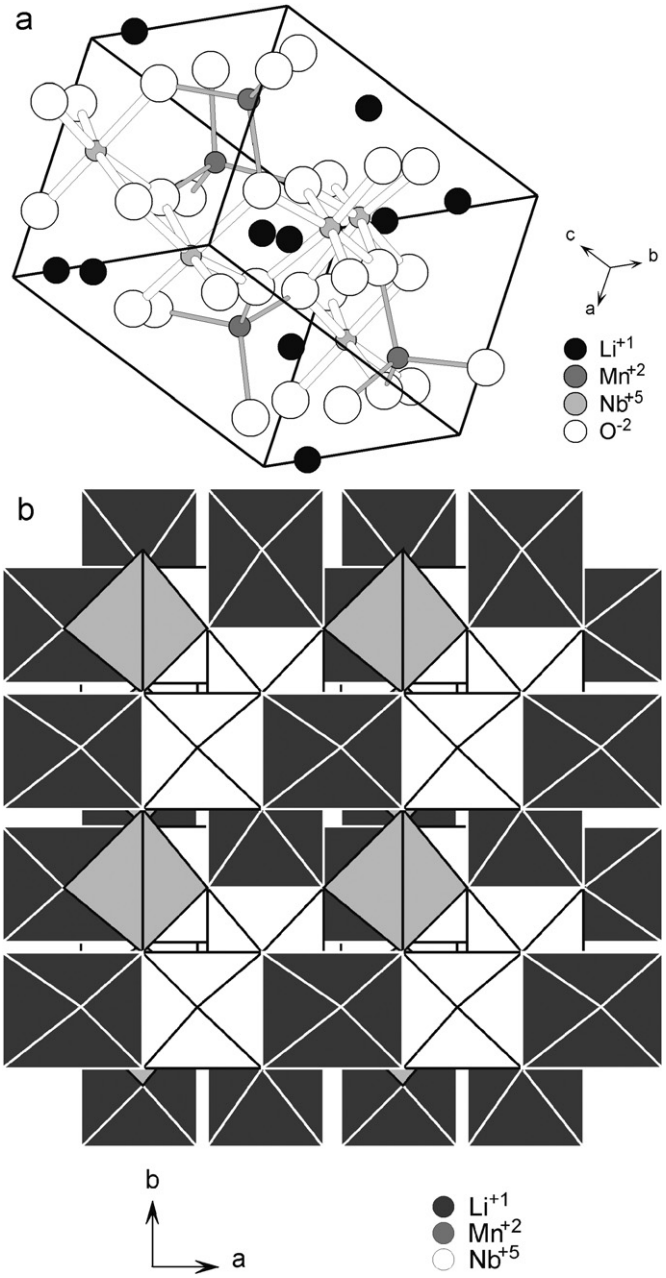

Fig. 2. Structure of $LiMnNbO_4$: (a) ball-and-stick model of the unit cell (Li–O bonds are not shown); (b) polyhedral representation (along the screw axis).

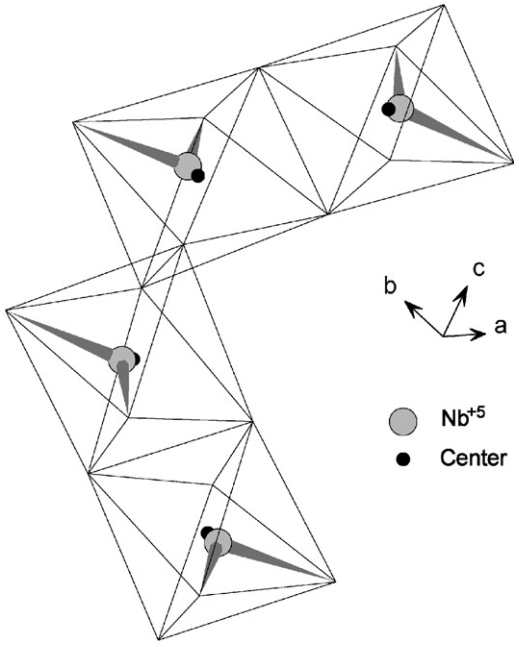

Fig. 3. Niobium displacement in NbO_4 chain. Two shortest Nb–O bonds are shown; weighted centre of coordinating oxygen positions is black.

any, degree of Li–Mn disordering. The final results are presented in Tables 2–4. The mean M–O distances agree with ionic radii sums.

The March–Dollase texture parameter ($R_o = 0.9905$) corresponds to platy crystals packing [9] but is very near to the no preferred orientation case ($R_o = 1$).

The quality of structure refinement was also verified by bond valence sum calculations. They were performed using function $v_{ij} = \exp((d_{ij}-L)/b)$, where v_{ij} is a valence of bond with j neighbour of i position, d_{ij}—distance between positions, $b = 0.37$ Å, L—unit bond length [13]. Table 5 shows good agreement between formal valences and calculated bond valence sums for all positions of structure.

3.3. Description of the structure

The most rigid fragments are NbO_4 chains extending along the screw axis 4_3 (Fig. 2). They consist of NbO_6 octahedra sharing two non-adjacent and non-parallel edges. The shared edges have shortened length and central

Table 6
Niobium acentrism in its coordination octahedra

Substance	Point group	Mean dist. (Å)	Mean dist. sigma (Å)	Center displ. (Å)	Minor angles (deg)	Displ. kind	Refs.
$LiNbO_3$	3	2.003	0.127	0.275	74.4, 76.4, 79.4	F	[14]
$LiNb_3O_8$	1	1.994	0.106	0.260	35.6, 58.9, 61.2	EF	[15]
	1	2.012	0.153	0.336	37.2, 50.3, 87.7	VE	
	1	2.017	0.161	0.344	27.1, 58.8, 87.7	VE	
Li_3NbO_4	3m	1.994	0.136	0.299	53.1, 53.1, 53.1	F	[16]
$LiZnNbO_4$	2	1.997	0.107	0.243	44.7, 44.7, 93.6	E	[5]
$Mn_4Nb_2O_9$	3	2.015	0.113	0.364	75.2, 75.2, 79.8	F	[11]
$MnNb_2O_6$	1	2.020	0.162	0.334	35.6, 38.0, 86.3	E	[12]
$Zn_3Nb_2O_8$	1	2.023	0.135	0.319	18.3, 49.4, 82.9	VE	[17]
$LiMnNbO_4$	2	1.988	0.128	0.243	45.1, 45.2, 92.1	E	This work

Radii sum for ^{VI}Nb–^{IV}O bond: 0.78 + 1.24 Å = 2.02 Å [7].
V, *E*, *F*—displacement towards one vertex, two vertices (edge) and three vertices (face), minor angles correspond to three nearest neighbours.

angle. The point symmetry of metals position is 2. Hence, they may be displaced from the weight centres of their oxygen coordination groups. The Nb^{+5} displacement (0.240 Å, see Fig. 3) is typical of the acentric positions of this element in oxygen octahedra (see related compounds in Table 6) and corresponds to its electronic configuration d^0 [18,19].

Both oxygen positions have distorted tetrahedral surrounding. O_1 has one Nb neighbour (with the shortest Nb–O bond 1.836 Å), one Mn (2.063 Å) and two Li. O_2 has two Nb neighbours (1.957 and 2.150 Å), one Mn (2.057 Å) and one Li.

4. Conclusion

A new compound $LiMnNbO_4$ has been prepared in reducing atmosphere. It is essentially stoichiometric, with no solid solution range. According to XRD powder profile analysis, it has a spinel-derived structure (space group $P4_122$ or $P4_322$) with Li and Nb ordered on octahedral sites and Mn on tetrahedral sites, and is isostructural with $LiZnNbO_4$. Li/Mn inversion is negligible.

Acknowledgments

This work was supported by the ICDD Grant-in-Aid program. The authors thank Dr. S.N. Polyakov who performed the Geigerflex scan and Dr. V.B. Nalbandyan for critical reading the manuscript.

References

[1] G. Blasse, J. Inorg. Nucl. Chem. 25 (1963) 230–232.
[2] M.E. Villafuerte-Castrejon, J.A. Azamar-Barrios, P. Bartolo-Perez, J. Solid State Chem. 140 (1998) 168–174.
[3] S.J. Marin, M. O'Keeffe, D.E. Partin, J. Solid State Chem. 113 (1994) 413–419.
[4] C. Gonzalez, M.L. Lopez, M. Gaitan, M.L. Veiga, C. Pico, Mater. Res. Bull. 29 (1994) 903–910.
[5] M. Ferriol, S. Lecocq, Eur. J. Solid State Inorg. Chem. 35 (1998) 707–714.
[6] V.B. Nalbandyan, B.S. Medvedev, V.I. Nalbandyan, A.V. Chinenova, Inorg. Mater. 24 (1988) 980–983 (in Russian).
[7] R.D. Shannon, Acta Cryst. A 32 (1976) 751–767.
[8] B.H. Toby, J. Appl. Cryst. 34 (2001) 210–230.
[9] A.C. Larson, R.B. von Dreele, General Structure Analysis System, Los Alamos National Laboratory Report LAUR 86-748, 2004.
[10] Powder diffraction File, ICDD, Release 2005.
[11] U. Rohweder, H.-K. Mueller-Buschbaum, J. Less-Comm. Metals. 138 (1988) 79–86.
[12] H. Weitzel, Z. Kristallogr. 144 (1976) 238–258.
[13] I.D. Brown, D. Altermatt, Acta Cryst. B 41 (1985) 244–247.
[14] R. Hsu, E.N. Maslen, D. du Boulay, Acta Cryst. B 53 (1997) 420–428.
[15] B.M. Gatehouse, P. Leverett, Cryst. Struct. Commun. 1 (1972) 83–86.
[16] K. Ukei, H. Suzuki, T. Shishido, T. Fukuda, Acta Cryst. C 50 (1994) 655–656.
[17] M. Isobe, F. Marumo, S. Iwai, Y. Kondo, Bull. Tokyo Inst. Technol. 120 (1974) 1–6.
[18] N.S.P. Bhuvanesh, J. Gopalakrishnan, J. Mater. Chem. 7 (1997) 2297–2306.
[19] K.M. Ok, S. Halasyamani, D. Casanova, M. Llunell, P. Alemany, S. Alvarez, Chem. Mater. 18 (2006) 3177–3183.